technologies

MDPI

Communication

Needleless Electrospinning of a Chitosan Lactate Aqueous Solution: Influence of Solution Composition and Spinning Parameters

Daria N. Poshina [1], Igor A. Khadyko [1,2], Arina A. Sukhova [1], Ilya V. Serov [3], Natalia M. Zabivalova [3] and Yury A. Skorik [1,*]

1 Institute of Macromolecular Compounds of the Russian Academy of Sciences, 199004 St. Petersburg, Russia; poschin@yandex.ru (D.N.P.); satrianin@gmail.com (I.A.K.); arina.a.s@mail.ru (A.A.S.)
2 Department of Biology, Ecology and Biotechnology, Northern (Arctic) Federal University named after M.V. Lomonosov, Severnaya Dvina emb. 17, 163001 Arkhangelsk, Russia
3 Inmed LLC, Svyazi str. 34A, Strelna, 198515 St. Petersburg, Russia; serovilya89@mail.ru (I.V.S.); nmzabivalova@nanofibers.ru (N.M.Z.)
* Correspondence: yury_skorik@mail.ru

Received: 30 November 2019; Accepted: 17 December 2019; Published: 19 December 2019

Abstract: The biological activity of chitosan determines its broad application as a biopolymer for non-woven wound dressings fabricated by electrospinning. The electrospinning process is affected by a large number of different factors that complicate its optimization. In the present work, the electrospinning of chitosan lactate was carried out using a needleless technique from water solutions of different compositions. Surface response methodology was used to evaluate the effects of the concentration of chitosan, polyethylene oxide, and ethanol on solution properties, such as viscosity, surface tension, and conductivity, as well as the process characteristics and fiber quality. The viscosity of the spinning solution is determined by the polymer concentration as well as by the interpolymer interactions. The addition of ethanol to the spinning solutions effectively decreases the solution surface tension and conductivity, while increasing the volatility of the solvent, to provide more intense fiber spinning. Atomic force microscopy revealed that the chitosan lactate fibers were obtained without defects and with a narrow thickness distribution. The spinning parameters, voltage, distance between electrodes, and rotation speed of the spinning electrode had insignificant influences on the fiber diameter during needleless electrospinning.

Keywords: chitosan lactate; non-woven materials; needleless electrospinning; response surface methodology

1. Introduction

Electrospun chitosan membranes have wide applications in biomedicine as wound dressings and in tissue regeneration and drug delivery [1–4] because of the biocompatibility, biodegradability, and biological activity of chitosan [5–7]. However, electrospinning of chitosan remains difficult: Only strongly acidic solutions can be spun effectively, and guest polymers (most frequently polyethylene oxide (PEO) or polyvinyl alcohol) must be used for initialization of the electrospinning process. Aqueous chitosan solutions are less stable than acidic ones and require greater initial amounts of PEO [8]. The process of electrospinning is influenced by many different factors, including the properties of the polymer solution, the parameters of the electrospinning process, and the environmental conditions [9]. The main properties of solutions that determine their spinning ability and affect the fiber quality are the viscosity, surface tension, and conductivity, and the solvent vapor volatility [10].

Electrospun fibers used for cell proliferation should have a diameter that corresponds to the size of the tissue extracellular matrix [11]. The fiber diameter also affects the mechanical properties of the electrospun membrane [12]. Fibers produced by an electrospinning process can, therefore, have diameters related to the process parameters [9] and to the properties of the initial polymers and their solutions [13]. The electrospinning process is frequently optimized by response surface methodology (RSM) [14–16], which allows determination of the influence of several factors and their interaction simultaneously by compact experiment design. RSM is, therefore, less time-consuming than the conventional one-factor-at-a-time approach [17,18] and can be used when the quantitative evaluation of response parameters is possible.

For a needle electrospinning process, a reverse relationship exists between the solution flow rate and the average fiber diameter [19]. The distance between the nozzle tip and the collector surface is also related to the diameter in cases of quick solvent evaporation [20]. By contrast, contradictory reports have been published on the role of the applied voltage on the diameter distribution. For example, Reneker et al. [21] indicated an inverse relationship, whereas Baumgarten et al. [22] reported a direct relationship, and Katti et al. [23] found no significant effect of voltage on the diameter distribution.

The main drawback of conventional needle electrospinning is a low yield of fibers. This has prompted the development of needleless electrospinning as a way to scale up fiber production. This higher productivity suggests the possibility of applying higher voltages of 30–70 kV as the solution volumes are increased. Needleless electrospinning has proven more advantageous when compared with multi-needle processes for scale-up [24]. For this process, Taylor cones and solution jets are formed next to each other on the surface of the rotating spinning electrode that emerges from the polymer solution. This technique differs from the conventional needle process and requires its own selection of optimal parameters. Therefore, identification of the dependencies that allow control over the process and the final quality of the nonwovens remains relevant.

The electrospinning of chitosan lactate has been described previously [25–27], but the procedure required the use of a high concentration of trifluoroacetic acid and methylene chloride, as well as the presence of polylactic acid as a guest polymer. In the present study, we report a "green" method that overcomes the usually poor spinning ability of chitosan lactate water solutions and allows needleless electrospinning of chitosan lactate fibers from an aqueous solution. The resulting electrospun mats from chitosan lactate became insoluble after heating due to crosslinking via amidation between chitosan and the lactate salt [28], making these fibers suitable for biomedical applications in water media.

The aims of the present study were to determine the effect of the spinning solution composition on the quality of the nanofibers obtained under the conditions of needleless electrospinning and to analyze the effect of adding ethanol as a way to increase the efficiency of electrospinning of chitosan from aqueous solutions.

2. Materials and Methods

2.1. Chitosan Characterization

Chitosan lactate was purchased from Biolog Heppe GmbH (Landsberg, Germany). The molecular weight (MW) and the degree of deacetylation (DD) were determined after neutralization of the chitosan lactate solution with NaOH followed by purification by dialysis and lyophilization. The MW of 8.0×10^4 was calculated from the Mark–Houwink equation [29]:

$$[\eta] = 3.41 \times 10^{-3} M_\eta{}^{1.02}, \quad (1)$$

where $[\eta]$ is the characteristic viscosity of a solution of chitosan in 2% acetic acid with 0.3 M NaCl, determined using an Ubbelohde capillary viscometer at a temperature of 20 °C and M_η is the viscosity average MW. The DD of chitosan sample was determined by conductometric titration (0.85) using a Hanna EC215 conductometer (Hanna Instruments, Woonsocket, RI, USA) and by ^{1}H NMR spectra

(0.86) recorded on a Bruker Avance 400 (Billerica, MA, USA) spectrometer at operating frequencies of 400 MHz. PEO with MW 9.0×10^5 was purchased from Merck Group (Darmstadt, Germany).

2.2. Electrospinning Solutions

A series of solutions were prepared to determine the influence of the solution composition and the process parameters. In the first case, the content of chitosan lactate, PEO, and ethanol was varied, as shown in Table 1. In the second case, the solution contained 3% chitosan lactate, 10% PEO (in relation to chitosan), and 10% ethanol. The chitosan lactate was first dissolved in water under stirring for 2 h. The calculated amount of PEO was then added, followed by the ethanol after the complete dissolution of the PEO. Ethanol was used to facilitate chitosan electrospinning from aqueous solutions, as these are characterized by high surface tension [30].

Table 1. Solution properties, electrospinning parameters, and fiber diameter depending on the solution composition.

Entry	Concentration, %			Solution Properties			E [1], kV/cm	Fiber Diameter, nm
	Chitosan Lactate (A)	PEO (B)	Ethanol (C)	η, mPa·s	σ, mN/m	Conductivity, mSm/cm		
1	4	20	10	6317	52.4	2.2	1.8	850 ± 110
2	4	5	0	781	65.4	3.2	2.4	500 ± 90
3	2	20	0	218	60.1	2.3	2.6	380 ± 70
4	2	5	10	210	48.0	1.7	2.3	470 ± 80

[1] E is the electric field intensity at which stable electrospinning occurred.

2.3. Determination of Solution Parameters

The dynamic viscosity (η) of the spinning solutions was determined using a Fungilab Viscolead Pro M (Fungilab, Barcelona, Spain) viscometer, the solution conductivity was determined using a Hanna EC 215 conductometer, and the surface tension (σ) was measured using a Krüss K20 tensiometer (Krüss GmbH, Hamburg, Germany).

2.4. Electrospinning

The electrospinning was performed using needleless NanoSpider Lab 500 equipment (Elmarco, Liberec, Czech Republic). The operating scheme is presented in Figure 1. The process parameters were maintained in the following intervals: voltage of 50–70 kV, the distance between electrodes of 20–24 cm, and rotating speed of 3–11 rpm.

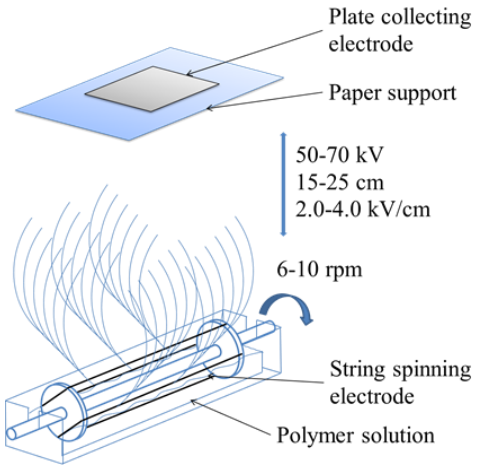

Figure 1. The NS Lab 500 non-capillary electrospinning unit (Elmarco, Czech Republic) and process parameters.

2.5. Fiber Morphology and Diameter

The morphology of the obtained fibers was studied by atomic force microscopy (AFM) using a Smena scanning probe microscope (NT-MDT, Zelenograd, Russia). Samples were scanned in tapping mode with a curvature tip radius of 10 nm, a probe resonant frequency of 190 kHz, and a force constant of 58 N/m. The processing of AFM images and the calculations of the average fiber diameters and standard deviations were performed using the ImageJ program. Scanning electron microscopy (SEM) was carried out on a Phenom G Pro instrument (Phenom-World BV, Eindhoven, the Netherlands), and the average fiber diameter and diameter distribution were determined using the microscope software.

2.6. Statistical Analysis

MS Excel with the statistical package was used for statistical analysis. A value of $p < 0.01$ was considered statistically significant for the model and the individual model terms.

3. Results and Discussion

3.1. The Influence of Solution Composition and Properties

Solutions for electrospinning were prepared according to the scheme of a fractional factorial design of 2^3 experiment, where the varied factors were the contents of chitosan (A), PEO (B), and ethanol (C). The solution parameters, the parameters of electrospinning, and the fiber diameters for given solution compositions are presented in Table 1. The intensity of the electric field during the stable electrospinning (E, kV/cm) was calculated from the applied voltage and used as a characteristic of the electrospinning process, taking into account the distance between the spinning and collector electrodes. The process parameters in each case were set optimally, based on a visual assessment of the intensity and quality of the electrospinning, and the minimum value of the voltage that gave high-quality spinning was recorded. In this case, the minimum voltage depends on the characteristics of the solutions. The values of the solution parameters mainly corresponded to the ranges suitable for electrospinning [10], with the exception of somewhat greater surface tension. The high surface tension of water is considered the main obstacle for its use as a solvent for polymers in electrospinning [10].

Table 2 shows the effects of each component on the defined parameters. An increase in the concentration of polymers caused a significant increase in the viscosity of the solutions, and an effect was also observed for the interaction of chitosan and PEO concentration, leading to an additional increase in viscosity. This latter effect is due to the interaction of the polymers through the formation of hydrogen bonds, which is considered as one of the reasons why PEO initiates the electrospinning of chitosan [31]. Increasing the chitosan concentration increased the conductivity of the solution, as well as its surface tension. The introduction of ethanol into the solution reduced these parameters, thereby increasing the spinnability of the solutions. An increase in the content of all the components resulted in a decrease in the spinning intensity, and the effect of increasing the concentration of chitosan exceeded the effect of increasing the content of PEO. The introduction of ethanol, to a great extent, facilitated the spinning process, but the possibility of an effect of the interaction of PEO and chitosan cannot be excluded.

Table 2. The influence of the solution composition on the solution properties and spinning process [1].

Component	Viscosity	Surface Tension	Conductivity	Intensity of the Stable Electrospinning	Fiber Diameter
Chitosan lactate (A)	++	+	++	−−	++
PEO (B)	++	0	−	−	+
Ethanol (C)	++ [2]	−−	−−	−− [2]	++ [2]

[1] +(−) modest influence, ++(−−) considerable influence, 0 neutral influence; [2] the effect is due to the conjugate effect of the interaction of the first two factors (AB).

An increase in the spinning voltage resulted in thinner fibers, and the effects of the content of the component solutions on tension and fiber thickness were inverse and in good agreement. In this case, an unambiguous characterization of the influence of the components of the solutions on the fiber sizes is not possible, but the solutions that were molded at low tension values can be used to regulate the fiber diameter in a rather wide range by changing the forming voltage. This dependence has been repeatedly reported in the literature [9].

3.2. Fiber Morphology

The AFM studies showed fibers that were smooth and free from beads (Figure 2) and with a rather narrow diameter distribution (Table 1). Overall, thinner fibers formed a denser network. A general consensus is that the diameter of the scaffold fibers for cell cultivation should correspond to the size of the fibers of the extracellular collagen matrix; that is, 50–500 nm [32]. Beads were observed rarely and only during the electrospinning of solution No 4 with minimal chitosan concentration and viscosity. Insufficient viscosity of the solution is considered to be one of the main reasons for the appearance of beads [33].

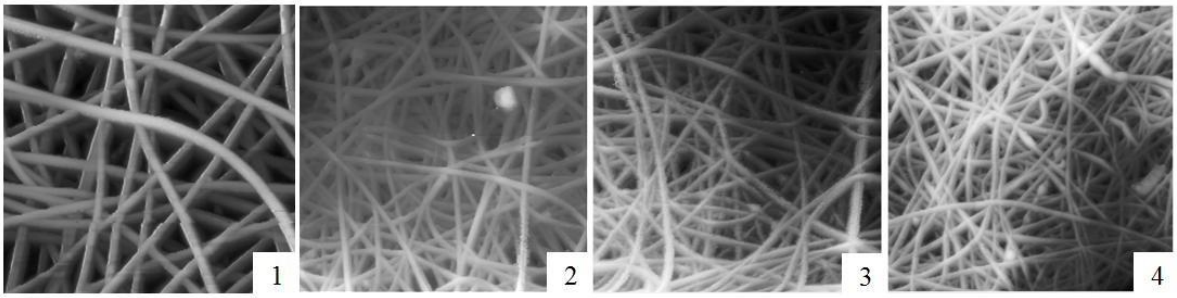

Figure 2. Atomic force microscopy (AFM) images of nanofibers electrospun from the solutions of different composition (presented in Table 1), scanning area size is 20 × 20 μm.

3.3. The Influence of Ethanol Addition

A series of experiments was carried out to determine the positive effect of ethanol on the efficiency of chitosan formation from aqueous media and to establish the optimal concentration of ethanol in the spinning solution (Figure 3). A qualitative decrease in the spinning efficiency was observed when 20 vol% of ethanol was added to the mixture; no further improvement occurred above this concentration.

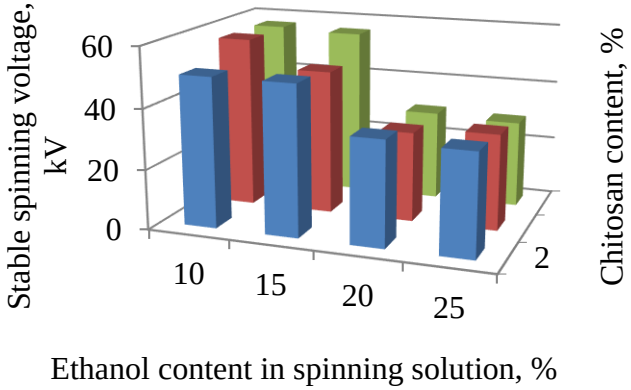

Figure 3. The influence of the ethanol addition on the electrospinning process.

3.4. The Influence of the Process Parameters

The RSM is used widely for the optimization of electrospinning processes. A study on the process of fabrication of magnetic nanofibers of polyvinyl alcohol incorporated with γ-Fe_2O_3 nanoparticles

distinguished only two significant parameters: flow rate and applied voltage [15]. RSM revealed the chitosan/PEO ratio and MW of chitosan as the main factors influencing the variation of accessible surface nitrogen concentrations between 0% and 6.4%. The model showed good adequacy, thereby providing a tool for tailoring the surface properties of chitosan/PEO blends by addressing the amount of accessible chitosan [14].

A full factorial design (2^3) was selected to screen out the process parameters. Appropriate levels for the parameters were determined by conducting some initial experiments to test the validity of all factorial points. Table 3 summarizes the factors and levels for factorial design during electrospinning.

Table 3. Factors and levels for full factorial design.

Factor	Low (−1)	Center (0)	High (+1)
Voltage (A, kV)	50	60	70
Distance (B, cm)	20	22	24
Rotating speed (C, rpm)	3	7	11

Statistical analyses were carried out for two response parameters: average fiber diameter and average electrical current during electrospinning. The current value was supposed to indicate the efficiency of electrospinning, similar to the electrical field intensity during the determination of solution influence on fiber diameter (see Section 3.1). The design layout and experimental results are presented in Table 4.

Table 4. Complete design layout and experimental results.

Entry	Run Order	U, kV	d, cm	ω, rpm	Fiber Diameter, nm				Current, μA
					AFM		SEM		
					Mica	Paper Support	Average	Mode	
1	3	70	24	11	350 ± 80	510 ± 70	286	244	32.5
2	7	70	24	3	460 ± 75	500 ± 65	271	253	34.5
3	8	70	20	11	455 ± 60	475 ± 70	242	228	40.0
4	6	70	20	3	380 ± 70	510 ± 50	279	251	47.0
5	4	50	24	11	530 ± 105	530 ± 70	279	227	12.0
6	2	50	24	3	310 ± 90	555 ± 90	307	282	14.5
7	1	50	20	11	200 ± 50	500 ± 85	260	235	22.0
8	5	50	20	3	400 ± 75	560 ± 60	290	199	14.0

The average fiber diameter was measured by several different methods. Fiber electrospinning directly to mica allowed the generation of fiber images that show greater detail (Figure 4), and that allowed the evaluation of the fiber diameter by the height of the fibers. However, the results differed substantially from the determinations of fiber width using SEM and AFM images because of the significantly smaller number of fibers on mica used in the calculations; therefore, the fiber height was not considered as a response parameter.

The fiber diameters obtained with AFM were two times larger than those obtained with SEM; however, the tendency of the changes was the same. The size difference can be related to the systematic error of the determination of fiber borders by the programs used. The model significance was determined for an average fiber diameter calculated from SEM images (Table 5), fiber diameter mode (Table 6), and average current (Table 7). The influence of a factor was considered significant at $p < 0.01$ [15].

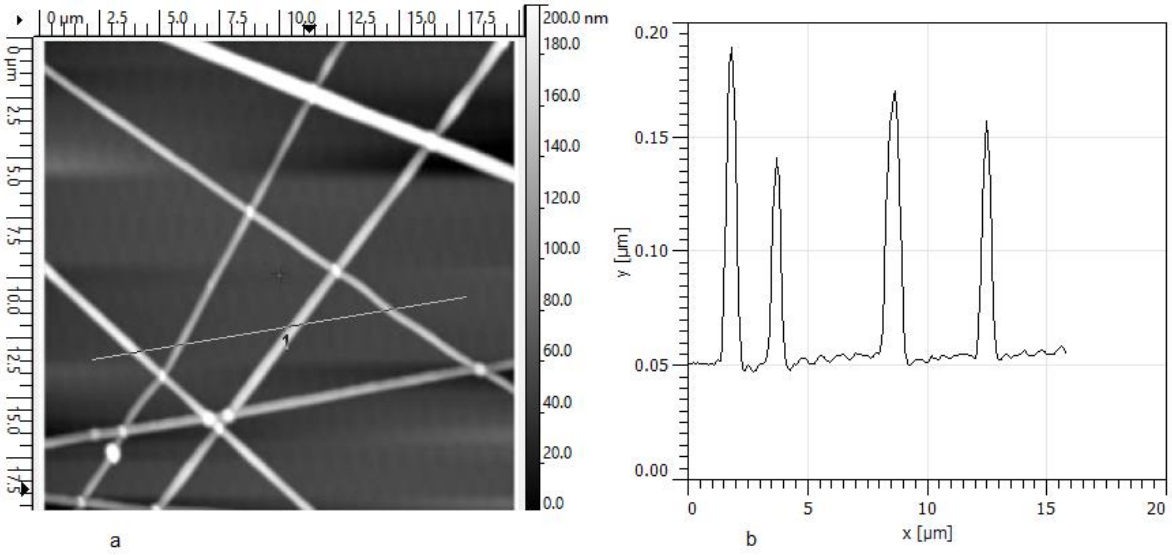

Figure 4. Chitosan fibers electrospun on mica (**a**) and their height profile (**b**).

Table 5. ANOVA analysis for average fiber diameter (SEM) as a response.

Source	df	Sum of Squares	Mean Square	F-Value	*p*-Value	Status
linear	3	1869	623	2.97	0.160	insignificant
a (U, kV)	1	421	421	2.00	0.230	insignificant
b (d, cm)	1	648	648	3.09	0.154	insignificant
c (ω, rpm)	1	800	800	3.81	0.123	insignificant
error	4	839	210			
total	7	2708				

Table 6. ANOVA analysis for fiber diameter mode (SEM) as a response.

Source	df	Sum of Squares	Mean Square	F-Value	*p*-Value	Status
linear	3	1520	507	0.81	0.552	insignificant
a (U, kV)	1	132	132	0.21	0.670	insignificant
b (d, cm)	1	1070	1070	1.70	0.262	insignificant
c (ω, rpm)	1	319	319	0.51	0.515	insignificant
error	4	2512	628			
total	7	4032				

Table 7. ANOVA analysis for average electrical current as a response.

Source	df	Sum of Squares	Mean Square	F-Value	*p*-Value	Status
linear	3	1157	386	20.88	0.007	significant
a (U, kV)	1	1047	1047	56.66	0.002	significant
b (d, cm)	1	109	109	5.89	0.072	insignificant
c (ω, rpm)	1	1.53	1.53	0.08	0.788	insignificant
error	4	73.9	18.5			
total	7	1231				

None of the models was statistically significant. The electrical current depends strongly on the applied voltage (or, more accurately, on the electrical field intensity) and does not depend on any other parameter that was varied during the experiment. Thus, the current is most likely related to the charges formed by ionization of the air close to the spinning electrode and the polymer jet [34]. Therefore, the current value cannot be considered as an indicator of electrospinning efficiency. The process

parameters used in needleless electrospinning of aqueous chitosan lactate did not have any significant influence on the fiber diameter.

4. Conclusions

Using the technique of surface response, we showed that the addition of ethanol to the composition of the spinning solutions greatly facilitates the process of electrospinning of chitosan from aqueous solutions because this addition decreases the surface tension and conductivity of the solution. The interaction of chitosan and PEO in spinning solutions affects the solution viscosity and spinning ability. The spinning process parameters during needleless electrospinning at high voltages of 50–70 kV have an insignificant influence on the fiber diameter.

Author Contributions: Conceptualization, D.N.P.; methodology, D.N.P.; investigation, D.N.P., I.A.K., A.A.S., I.V.S. and N.M.Z.; writing—original draft preparation, D.N.P.; writing—review and editing, Y.A.S.; supervision, Y.A.S.; funding acquisition, Y.A.S. All authors have read and agreed to the published version of the manuscript.

Funding: This research was funded by the Russian Foundation for Basic Research, projects 18-29-17074 (D.N.P., A.A.S., Y.A.S.), 19-33-50022 (I.A.K., Y.A.S.).

Acknowledgments: The authors are grateful to INMED LLC (CEO A.V. Vnuchkin) for providing the NanoSpider NS Lab 500 equipment for this work to be performed.

Conflicts of Interest: The authors declare no conflict of interest. The funders had no role in the design of the study; in the collection, analyses, or interpretation of data; in the writing of the manuscript, or in the decision to publish the results.

References

1. Qasim, S.B.; Zafar, M.S.; Najeeb, S.; Khurshid, Z.; Shah, A.H.; Husain, S.; Rehman, I.U. Electrospinning of chitosan-based solutions for tissue engineering and regenerative medicine. *Int. J. Mol. Sci.* **2018**, *19*, 407. [CrossRef] [PubMed]
2. Bossard, F.; Rinaudo, M. Biomaterials from chitosan processed by electrospinning. *Nano World J.* **2019**, *5*, 33–36. [CrossRef]
3. Kalantari, K.; Afifi, A.M.; Jahangirian, H.; Webster, T.J. Biomedical applications of chitosan electrospun nanofibers as a green polymer—Review. *Carbohydr. Polym.* **2019**, *207*, 588–600. [CrossRef] [PubMed]
4. Petrova, V.A.; Chernyakov, D.D.; Poshina, D.N.; Gofman, I.V.; Romanov, D.P.; Mishanin, A.I.; Golovkin, A.S.; Skorik, Y.A. Electrospun bilayer chitosan/hyaluronan material and its compatibility with mesenchymal stem cells. *Materials* **2019**, *12*, 2016. [CrossRef]
5. Younes, I.; Rinaudo, M. Chitin and chitosan preparation from marine sources. Structure, properties and applications. *Mar. Drugs* **2015**, *13*, 1133–1174. [CrossRef]
6. Cheung, R.C.F.; Ng, T.B.; Wong, J.H.; Chan, W.Y. Chitosan: An update on potential biomedical and pharmaceutical applications. *Mar. Drugs* **2015**, *13*, 5156–5186. [CrossRef]
7. Poshina, D.N.; Raik, S.V.; Poshin, A.N.; Skorik, Y.A. Accessibility of chitin and chitosan in enzymatic hydrolysis: A review. *Polym. Degrad. Stab.* **2018**, *156*, 269–278. [CrossRef]
8. Mengistu Lemma, S.; Bossard, F.; Rinaudo, M. Preparation of pure and stable chitosan nanofibers by electrospinning in the presence of poly(ethylene oxide). *Int. J. Mol. Sci.* **2016**, *17*, 1790. [CrossRef]
9. Haider, A.; Haider, S.; Kang, I.-K. A comprehensive review summarizing the effect of electrospinning parameters and potential applications of nanofibers in biomedical and biotechnology. *Arab. J. Chem.* **2015**, *11*, 1165–1188. [CrossRef]
10. Prokopchuk, N.R.; Shashok, Z.S.; Prishchepenko, D.V.; Melamed, V.D. Nanofibres electrospinning from chitosan solutions (a review). *Polimernye Materialy I Tekhnologii* **2015**, *1*, 36–56.
11. Jun, I.; Han, H.-S.; Edwards, J.R.; Jeon, H. Electrospun fibrous scaffolds for tissue engineering: Viewpoints on architecture and fabrication. *Int. J. Mol. Sci.* **2018**, *19*, 745. [CrossRef] [PubMed]
12. Baji, A.; Mai, Y.-W.; Wong, S.-C.; Abtahi, M.; Chen, P. Electrospinning of polymer nanofibers: Effects on oriented morphology, structures and tensile properties. *Compos. Sci. Technol.* **2010**, *70*, 703–718. [CrossRef]
13. Berry, C.C. Progress in functionalization of magnetic nanoparticles for applications in biomedicine. *J. Phys. D Appl. Phys.* **2009**, *42*, 224003. [CrossRef]

14. Bosiger, P.; Richard, I.M.T.; Le Gat, L.; Michen, B.; Schubert, M.; Rossi, R.M.; Fortunato, G. Application of response surface methodology to tailor the surface chemistry of electrospun chitosan-poly(ethylene oxide) fibers. *Carbohydr. Polym.* **2018**, *186*, 122–131. [CrossRef] [PubMed]
15. Ahmadipourroudposht, M.; Fallahiarezoudar, E.; Yusof, N.M.; Idris, A. Application of response surface methodology in optimization of electrospinning process to fabricate (ferrofluid/polyvinyl alcohol) magnetic nanofibers. *Mater. Sci. Eng. C* **2015**, *50*, 234–241. [CrossRef] [PubMed]
16. Montgomery, D.C. *Design and Analysis of Experiments*; John Wiley & Sons: Hoboken, NJ, USA, 2017; p. 752.
17. Noordin, M.Y.; Venkatesh, V.C.; Chan, C.L.; Abdullah, A. Performance evaluation of cemented carbide tools in turning aisi 1010 steel. *J. Mater. Process. Technol.* **2001**, *116*, 16–21. [CrossRef]
18. Thiele, J.D.; Melkote, S.N. Effect of cutting edge geometry and workpiece hardness on surface generation in the finish hard turning of aisi 52100 steel. *J. Mater. Process. Technol.* **1999**, *94*, 216–226. [CrossRef]
19. Sung, Y.K.; Ahn, B.W.; Kang, T.J. Magnetic nanofibers with core (fe3o4 nanoparticle suspension)/sheath (poly ethylene terephthalate) structure fabricated by coaxial electrospinning. *J. Magn. Magn. Mater.* **2012**, *324*, 916–922. [CrossRef]
20. Sukigara, S.; Gandhi, M.; Ayutsede, J.; Micklus, M.; Ko, F. Regeneration of bombyx mori silk by electrospinning. Part 2. Process optimization and empirical modeling using response surface methodology. *Polymer* **2004**, *45*, 3701–3708. [CrossRef]
21. Reneker, D.H.; Kataphinan, W.; Theron, A.; Zussman, E.; Yarin, A.L. Nanofiber garlands of polycaprolactone by electrospinning. *Polymer* **2002**, *43*, 6785–6794. [CrossRef]
22. Baumgarten, P.K. Electrostatic spinning of acrylic microfibers. *J. Colloid Interface Sci.* **1971**, *36*, 71–79. [CrossRef]
23. Katti, D.S.; Robinson, K.W.; Ko, F.K.; Laurencin, C.T. Bioresorbable nanofiber-based systems for wound healing and drug delivery: Optimization of fabrication parameters. *J. Biomed. Mater. Res. Part B Appl. Biomater.* **2004**, *70*, 286–296. [CrossRef]
24. Begum, H.A.; Khan, M.K.R. Study on the various types of needle based and needleless electrospinning system for nanofiber production. *Int. J. Text. Sci.* **2017**, *6*, 110–117.
25. Cheng, T.; Hund, R.D.; Aibibu, D.; Horakova, J.; Cherif, C. Pure chitosan and chitsoan/chitosan lactate blended nanofibres made by single step electrospinning. *Autex Res. J.* **2013**, *13*, 128–133. [CrossRef]
26. Nguyen, T.T.T.; Chung, O.H.; Park, J.S. Coaxial electrospun poly(lactic acid)/chitosan (core/shell) composite nanofibers and their antibacterial activity. *Carbohydr. Polym.* **2011**, *86*, 1799–1806. [CrossRef]
27. Shan, X.; Li, F.; Liu, C.; Gao, Q. Electrospinning of chitosan/poly(lactic acid) nanofibers: The favorable effect of nonionic surfactant. *J. Appl. Polym. Sci.* **2014**, *131*. [CrossRef]
28. Cooper, A.; Bhattarai, N.; Kievit, F.M.; Rossol, M.; Zhang, M. Electrospinning of chitosan derivative nanofibers with structural stability in an aqueous environment. *Phys. Chem. Chem. Phys.* **2011**, *13*, 9969–9972. [CrossRef]
29. Pogodina, N.V.; Pavlov, G.M.; Bushin, S.V.; Mel'nikov, A.B.; Lysenko, Y.B.; Nud'ga, L.A.; Marsheva, V.N.; Marchenko, G.N.; Tsvetkov, V.N. Conformational characteristics of chitosan molecules as demonstrated by diffusion-sedimentation analysis and viscometry. *Polym. Sci. USSR* **1986**, *28*, 251–259. [CrossRef]
30. Sonina, A.N.; Uspenskii, S.A.; Vikhoreva, G.A.; Filatov, Y.N.; Gal'braikh, L.S. Production of nanofibre materials from chitosan by electrospinning (review). *Fibre Chem.* **2011**, *42*, 350–358. [CrossRef]
31. Pakravan, M.; Heuzey, M.-C.; Ajji, A. A fundamental study of chitosan/peo electrospinning. *Polymer* **2011**, *52*, 4813–4824. [CrossRef]
32. Ma, P.X.; Zhang, R. Synthetic nano-scale fibrous extracellular matrix. *J. Biomed. Mater. Res.* **1999**, *46*, 60–72. [CrossRef]
33. Fong, H.; Chun, I.; Reneker, D.H. Beaded nanofibers formed during electrospinning. *Polymer* **1999**, *40*, 4585–4592. [CrossRef]
34. Yalcinkaya, B.; Yener, F.; Jirsak, O.; Cengiz-Callioglu, F. On the nature of electric current in the electrospinning process. *J. Nanomater.* **2013**, *2013*, 538179. [CrossRef]